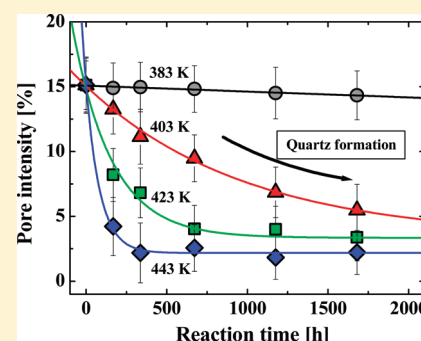


# Origin of Organism-Dependent Biogenic Silica Quartz Formation

Kiminori Sato\*

Department of Environmental Sciences, Tokyo Gakuai University, 4-1-1 Koganei, Tokyo 184-8501, Japan

**ABSTRACT:** Organism-dependent biogenic quartz formation in the steady-state environment is a phenomenon that can address the global environmental issues such as diagenetic evolution, biogeochemical cycling, and reservoir formation, but detailed studies have not been performed so far. Here, steady-state quartz formation is studied for amorphous silica of different biogenic origin on the basis of the recently established mechanistic model [Sato et al., *J. Phys. Chem. C* **2011**, *115*, 18131]. Amorphous silica originated from rice husks possesses angstrom-scale pores larger by 1.3 Å than those originated from diatom algae. The slight difference of pore size dramatically reduces activation energies of water diffusion by 78% and reactions of water molecules at pore surfaces by 47%, resulting in the reduction of activation energy of biogenic quartz formation by 64%. The present findings evidence that angstrom-scale pores intrinsically residing in the amorphous matrix are the organism-dependent origin of steady-state biogenic quartz formation.



## INTRODUCTION

Biogenic silica ubiquitously present in nature originates from a wide variety of living organisms such as, e.g., diatom, radiolarian, silicoflagellate, siliceous sponge, and plant.<sup>1–3</sup> Diatoms, unicellular algae found in marine environments, may be largely responsible for the global scale for biogenic silica formation. Rice husk is an abundant agricultural waste, in which biogenic silica is easily produced. Upon the production of biogenic silica, organisms take up silicon to form well-defined silica structures in their skeletons, which is of particular importance in understanding global cycling of silicon.<sup>4</sup> In spite of an interest in the formation mechanism dependent on the organism, detailed studies have not been performed due to the difficulty in finding the characteristic signature of organism-dependent origin for structurally complex silica composed of contaminated light elements.

Experiments on aqueous solution have suggested the significance of microscopic local structures for the kinetics of mineral dissolution and precipitation.<sup>5,6</sup> Wang et al. observed the change of the surface acidity constant for alumina particles with decreasing the pore size down to nanometers, implying an enhancement of ion sorption on pore surfaces.<sup>5</sup> Dove et al. found that the kinetics of amorphous silica dissolution exhibits a strong exponential dependence on chemical-driving force, in which specific surface structures on the atomic scale have to be taken into account.<sup>6</sup> Recently, we succeeded in establishing the mechanistic model of biogenic quartz formation by directly probing angstrom-scale pores apart from aqueous solution.<sup>7</sup>

In this study, the steady-state formation of biogenic quartz arising from rice husks is investigated focusing on angstrom-scale pores. The mechanism of organism-dependent formation is highlighted along with the data of quartz formation on diatom algae on the basis of a recently established mechanistic

model.<sup>7</sup> The purpose of the present work is to answer the following fundamental questions: (1) Does biogenic silica quartz formation depend on organisms? (2) What is the origin of organism-dependent formation if any.

## EXPERIMENTAL SECTION

Rice husk ash originated from Niigata Koshihikari was employed in the present study. The ash was milled and subjected to high-temperature roasting to eliminate organic matters. A hydrothermal reaction on a 70-day time scale was performed to obtain amorphous silica in the temperature range from 383 to 443 K in a cylindrical Teflon vessel. Silica products were examined by X-ray diffraction (XRD).

The sizes of angstrom pores and their intensities were investigated by positron annihilation lifetime spectroscopy. A fraction of energetic positrons injected into samples forms the bound state with an electron, positronium (Ps). Singlet *para*-Ps (*p*-Ps) with the spins of the positron and electron antiparallel and triplet *ortho*-Ps (*o*-Ps) with parallel spins are formed at a ratio of 1:3. Hence, three states of positrons, *p*-Ps, *o*-Ps, and free positrons, exist in the samples. The annihilation of *p*-Ps results in the emission of two  $\gamma$ -ray photons of 511 keV with lifetime  $\sim 125$  ps. Free positrons are trapped by negatively charged parts such as polar elements and annihilated into two photons with lifetime  $\sim 450$  ps. The positron in *o*-Ps undergoes two-photon annihilation with one of the bound electrons with a lifetime of a few nanoseconds after localization in angstrom-scale pores. The last process is known as *o*-Ps pick off annihilation and provides information on the free volume size through its lifetime  $\tau_3$  based on the

Received: September 9, 2011

Revised: October 25, 2011

Published: October 25, 2011

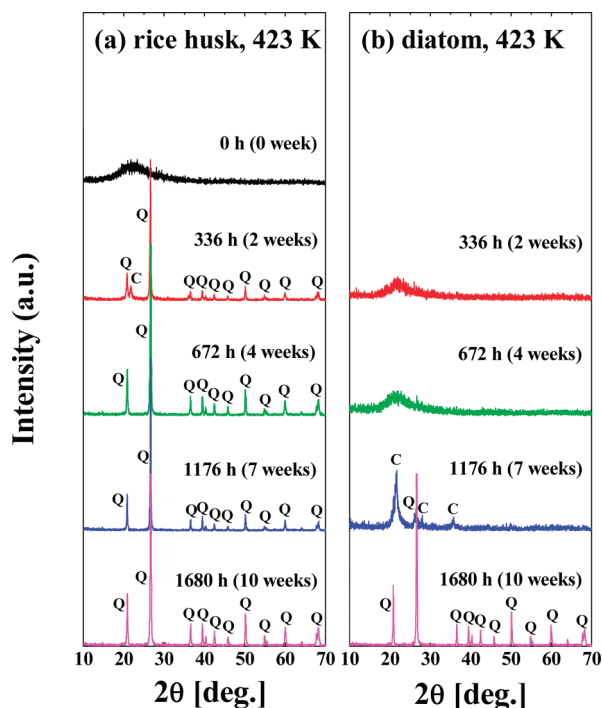


**Figure 1.** (a) X-ray diffraction patterns observed for rice husk-originated materials hydrothermally reacted at 423 K for 0 h (0 week), 336 h (2 weeks), 672 h (4 weeks), 1176 h (7 weeks), and 1680 h (10 weeks). XRD peaks indexed to cristobalite and quartz are marked with C and Q, respectively. The XRD data for diatom-originated materials taken from the literature<sup>7</sup> are added as (b) for comparison.

Tao–Eldrup model<sup>8,9</sup>

$$\tau_3 = 0.5 \left[ 1 - \frac{R}{R_0} + \frac{1}{2\pi} \sin\left(\frac{2\pi R}{R_0}\right) \right]^{-1} \quad (1)$$

where  $R_0 = R + \Delta R$  and  $\Delta R = 0.166$  nm is the thickness of the homogeneous electron layer in which the positron in *o*-Ps annihilates. The positron source (<sup>22</sup>Na), sealed in a thin foil of Kapton, was mounted in a sample–source–sample sandwich. The positron lifetime spectra were numerically analyzed using the POSITRONFIT code.<sup>10</sup>

Pore surfaces were investigated by means of momentum distributions of *o*-Ps pick-off annihilation localized at angstrom-scale pores. This momentum spectroscopy is based on the principle that if the positron–electron annihilation accompanies a longitudinal momentum  $p$  the resulting annihilation  $\gamma$ -rays are Doppler shifted from  $m_0c^2$  by  $\pm cp/2$ . Here,  $m_0$  and  $c$  are the electron rest mass and velocity of light, respectively. Measurements of the Doppler shifts by  $\gamma$ -ray energy spectroscopy with a high-purity Ge detector make it possible to obtain information on the momentum distribution of the positron–electron annihilation pairs. The momentum distribution of *o*-Ps is broadened and centered at 511 keV because the pick-off annihilation is influenced by electrons bound to the surrounding molecules.<sup>11,12</sup> Thus, the momentum distribution of *o*-Ps pick-off annihilation provides the information on the electronic states of angstrom-scale pore surfaces. The momentum distribution of *o*-Ps pick-off annihilation was extracted by time-resolved momentum measurements of positron–electron annihilation photons using recently developed

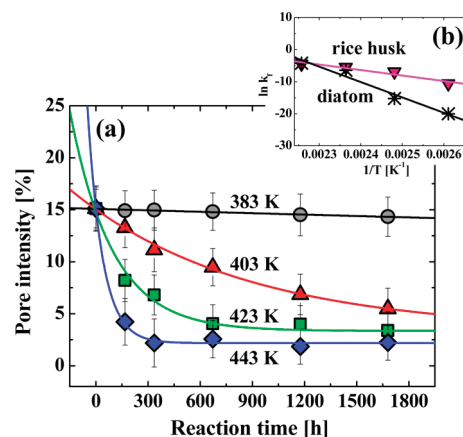


**Figure 2.** (a) Reaction-time variations of pore intensities at 383 K (gray circles), 403 K (red triangles), 423 K (green squares), and 443 K (blue diamonds) observed for rice husk-originated materials. Solid lines denote the results of the fits by an exponential with a decay constant  $k_f$ . (b) Logarithms of decay constants as a function of inverse temperature obtained for the rice husk-originated materials (pink inverse triangles). The data for diatom-originated materials taken from the literature<sup>7</sup> are added as stars for comparison.

positron-age-momentum correlation (AMOC) spectroscopy.<sup>13</sup> Taking the ratio of the central area over  $(-3.6 \text{ to } +3.6) \times 10^{-3} m_0c$  to the total area of the momentum spectrum, *o*-Ps pick-off annihilation was parametrized.<sup>14</sup> We call it pore-surface parameter that was recently found to be sensitive to light elements on pore surfaces such as, e.g., oxygen.<sup>7,13</sup>

## RESULTS AND DISCUSSION

Figure 1 (a) shows XRD patterns observed for the rice husk-originated materials reacted at 423 K for 0 h (0 week), 336 h (2 weeks), 672 h (4 weeks), 1176 h (7 weeks), and 1680 h (10 weeks). The data for the diatom-originated materials taken from the literature<sup>7</sup> are presented as (b) for comparison. Structural evolution toward crystalline quartz with the reaction time can be seen in the variation for both the materials. The diffraction pattern exhibits a typical amorphous structure for the rice husk-originated material at 0 h. XRD peaks arising from the quartz phase begin to appear together with those from the cristobalite phase at 336 h. The peaks of cristobalite phase disappear at 672 h, and the quartz phase is dominantly formed thereafter. The same sequential reactions take place for the diatom-originated materials but starts at 1176 h largely later than for the rice husk-originated materials. This demonstrates that biogenic quartz formation for rice husk-originated materials occurs more easily than for the diatom-originated materials.

Positron lifetime spectroscopy for the diatom- and rice husk-originated amorphous silica yields three components of lifetimes, of which the longest-lived component is attributable to the pick-off annihilation of *o*-Ps localized in the angstrom-scale pores of the amorphous matrix. The *o*-Ps lifetimes obtained for the diatom- and rice husk-originated amorphous silica are 1.6 and 3.1 ns corresponding to the pore sizes of 2.4 and 3.7 Å in radius, respectively. Note that the pore size for the rice husk-originated amorphous silica is slightly larger by 1.3 Å than for the diatom-originated amorphous silica. No systematic changes are observed in the lifetime  $\tau_3$  for both the materials when the quartz formation proceeds at longer reaction time. In light of the fact that

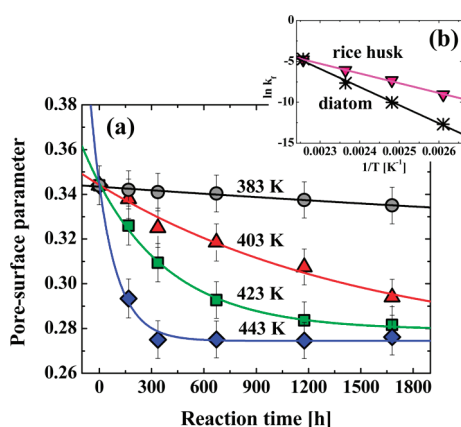


**Figure 3.** (a) Reaction-time variations of pore-surface parameter at 383 K (gray circles), 403 K (red triangles), 423 K (green squares), and 443 K (blue diamonds). Solid lines denote the results of the fits by an exponential with a decay constant  $k_f$ . (b) Logarithms of decay constants as a function of inverse temperature obtained for the rice husk-originated materials (pink inverse triangles). The data for diatom-originated materials taken from the literature<sup>7</sup> are added as stars for comparison.

no long lifetime component  $\tau_3$  is observed in silica polymorphs with high crystallinity, such as, e.g., crystalline quartz,<sup>15</sup> angstrom-scale pores are located not in the quartz phase but in the intergranular amorphous regions.

Figure 2(a) shows reaction-time variations of pore intensities at 383, 403, 423, and 443 K for the rice husk-originated materials. The pore intensities decrease with increasing the reaction time up to 1680 h (10 weeks). The decreasing tendency with the reaction time becomes increasingly prominent when the temperature is raised up to 443 K. The quartz formation in the amorphous matrix creates the intergranular amorphous regions, and its growth reduces the volume fraction of intergranular amorphous regions. It is thus reasonable that angstrom-scale pores in the intergranular amorphous regions decrease together with the quartz formation.

The quartz formation can now be visible with respect to the structural modification of silica itself apart from aqueous solution. Good fits of isotherms are obtained by an exponential with a decay constant  $k_f$ , as indicated with solid lines in Figure 2 (a). In Figure 2 (b), the logarithms of decay constants are plotted as a function of inverse temperature. It follows the Arrhenius law demonstrating that the quartz formation is governed by the thermally activated reaction. For comparison, the data of diatom-originated materials<sup>7</sup> are presented as stars, which indicates a steeper gradient than for the rice husk-originated materials. From the temperature variations, the activation energies of quartz formation are derived to be 1.5 and 4.2 eV for the rice husk- and diatom-originated materials, respectively, consistent with the XRD data of Figure 1.

Pore-surface parameters at 383, 403, 423, and 443 K for the rice husk-originated materials are shown in Figure 3 (a) as a function of reaction time. As is detailed in our earlier papers,<sup>7,13</sup> the decrease of pore-surface parameters with increasing reaction time is a consequence resultant from increased oxygen atoms incorporated with pore surfaces. The thermally activated reactions of water molecules at pore surfaces are well seen. The logarithms of the decay constants obtained from an exponential fit are plotted as a function of inverse temperature together with those of diatom-originated materials in Figure 3 (b). Similarly to

**Table 1.** Activation Energies of Quartz Formation  $E_f$ , Water Diffusion through Angstrom-Scale Pores  $E_d$ , and Water Reaction at Pore Surfaces  $E_r$ <sup>a</sup>

organism	$r$ [Å]	$E_f$ [eV]	$E_d$ [eV]	$E_r$ [eV]
diatom	2.4	4.2	2.3	1.9
rice husk	3.7	1.5	0.5	1.0

<sup>a</sup> The average pore sizes in radius  $r$  are presented as well.

the case of quartz formation of Figure 2, Arrhenius plots for the diatom-originated materials indicate a steeper gradient than for the rice husk-originated materials, in which the activation energies of water reactions at pore surfaces are derived to be 1.0 and 1.9 eV for the rice husk- and diatom-originated materials, respectively.

Following our recent model that explains the steady-state formation of biogenic quartz by the mechanistic theory of nucleation taking account of diffusion and reactions of water molecules in angstrom-scale pores,<sup>7</sup> the temperature-dependent quartz formation rate  $J$  is described as

$$J(T) = A \exp\left(-\frac{E_f}{kT}\right) \quad (2)$$

where  $A$ ,  $T$ ,  $E_f$ , and  $k$  are a pre-exponential factor, temperature, the activation energy of quartz formation, and the Boltzmann constant, respectively. Being that diffusion of water molecules through angstrom-scale pores and reactions of water molecules at pore surfaces are involved in the quartz formation,<sup>6,7,16,17</sup> eq 2 is rewritten as

$$J(T) = A \exp\left(-\frac{E_d}{kT}\right) \exp\left(-\frac{E_r}{kT}\right) \quad (3)$$

where  $E_d$  and  $E_r$  are the activation energies of water diffusion through angstrom-scale pores and water reaction at pore surfaces, respectively. Table 1 lists  $E_f$ ,  $E_d$ , and  $E_r$  values determined by applying eqs 2 and 3 to the Arrhenius plots in Figures 2 (b) and 3 (b).

The activation energy of water diffusion  $E_d$  for the rice husk-originated materials is much lower than for the diatom-originated materials. As mentioned above, the pore size for the rice husk-originated materials is larger by 1.3 Å than for diatom-originated materials. The results thus demonstrate that water molecules more easily diffuse through larger pores in the rice husk-originated materials. According to first-principle calculations on amorphous silica,<sup>18</sup> the activation energy of water diffusion through angstrom-scale pores is 2.2 eV at the pore radius of 2 Å. It decreases down to 0.8 eV when the pore size is raised up to 3.5 Å. The activation energies for both the materials evaluated in the present study well coincide with the above calculation, thus ascertaining the validity of our model.<sup>7</sup>

The activation energy of water reaction  $E_r$  for the rice husk-originated materials is almost half of that of diatom-originated materials. This is in contrast with our speculation that the value of  $E_r$  for the rice husk-originated materials with larger pores is higher than for the diatom-originated materials owing to less interaction of water molecules with the silica network. First-principle calculation predicts that the concentration of water molecules becomes high in the pores larger than 6 Å and that water molecules significantly cluster together.<sup>19</sup> Water molecules thus react with each other forming  $\text{OH}^-$  and  $\text{H}_3\text{O}^+$  at



considerably low energy in the vicinity of pore surfaces, which exactly coincides with our case. We most probably expect that the low activation energy  $E_r$  obtained for the rice husk-originated materials is the consequence of mutual interaction among water molecules in the 3.7 Å pores.

Here, we describe the reason why the biogenic-quartz formation for the rice husk-originated materials occurs more easily than for the diatom-originated materials. The rice husk- and diatom-originated amorphous silica intrinsically possesses angstrom-scale pores with the sizes of 3.7 and 2.4 Å in amorphous matrices, respectively. Water molecules diffuse through the larger pores of rice husk-originated materials with the low activation energy of 0.5 eV. Water molecules easily reach pore surfaces to react thereon. In the larger pores of rice husk-originated materials, the concentration of water molecules becomes high, and clusters of water molecules are significantly formed. The reaction among water molecules at pore surfaces is thus rather significant compared to that between water molecules and the silica network resulting in the lower activation energy of 1.0 eV than expected. This triggers the nucleation of biogenic quartz involving the totally lower energy cost of 1.5 eV than for the diatom-originated materials.

## CONCLUSIONS

The steady-state formation of biogenic quartz is studied for amorphous silica originated from rice husks and diatom algae on the basis of the recently established mechanistic model.<sup>7</sup> Amorphous silica originated from rice husks and diatom algae possesses angstrom-scale pores with the size of 3.7 and 2.4 Å, respectively. The slightly large pores of rice husk-originated materials make activation energies of water diffusion and reactions of water molecules at pore surfaces lower than those of diatom-originated materials by 78% and 64%, respectively, thus resulting in the reduction of activation energy of quartz formation by 64%. The present findings evidence that angstrom-scale pores intrinsically residing in the amorphous matrix are the organism-dependent origin of steady-state biogenic quartz formation.

## AUTHOR INFORMATION

### Corresponding Author

\*E-mail: sato-k@u-gakugei.ac.jp.

## ACKNOWLEDGMENT

Discussion with Profs. Fujimoto (Tokyo Gakugei University), Nakata (Tokyo Gakugei University), and Shikazono (Keio University) is gratefully appreciated. This work was partially supported by a Grant-in-Aid of the Japanese Ministry of Education, Science, Sports and Culture (Grant Nos. 21540317 and 23740234).

## REFERENCES

- (1) Lowenstam, H. Minerals formed by organisms. *Science* **1981**, *211*, 1126–1131.
- (2) Mann, S.; Ozin, G. Synthesis of Inorganic Materials with Complex Form. *Nature* **1996**, *382*, 313–318.
- (3) Bansal, V.; Ahmad, A.; Sastry, M. Fungus-mediated biotransformation of amorphous silica in rice husk to nanocrystalline silica. *J. Am. Chem. Soc.* **2006**, *128*, 14059–14066.
- (4) Leng, M. J.; Swann, G. E. A.; Hodson, M. J.; Tyler, J. J.; Patwardhan, S. V.; Sloane, H. The potential use of silicon isotope

composition of biogenic silica as a proxy for environmental change. *Silicon* **2009**, *1*, 65–77.

- (5) Wang, Y.; Bryan, C.; Xu, H.; Gao, H. Nanogeochemistry: Geochemical Reactions and Mass Transfers In Nanopores. *Geology* **2003**, *31*, 387–390.

- (6) Dove, P. M.; Han, N.; Wallace, A. F.; De Yoreo, J. J. Kinetics of amorphous silica dissolution and the paradox of the silica polymorphs. *Proc. Natl. Acad. Sci. U.S.A.* **2008**, *105*, 9903–9908.

- (7) Sato, K.; Fujimoto, K.; Nakata, M.; Hatta, T. Diffusion-Reaction of Water Molecules in Angstrom Pores as Basic Mechanism of Biogenic Quartz Formation. *J. Phys. Chem. C* **2011**, *115*, 18131–18135.

- (8) Tao, S. J. Positronium annihilation in molecular substances. *J. Chem. Phys.* **1972**, *56*, 5499–5510.

- (9) Eldrup, M.; Lightbody, D.; Sherwood, J. N. The temperature dependence of positron lifetimes in solid pivalic acid. *Chem. Phys.* **1981**, *63*, 51–58.

- (10) Kirkegaard, P.; Eldrup, M. Positronfit extended: A new version of a program for analysing position lifetime spectra. *Comput. Phys. Commun.* **1974**, *7*, 401–409.

- (11) Sato, K.; Ito, K.; Hirata, K.; Yu, R. S.; Kobayashi, Y. Intrinsic momentum distributions of positron and positronium annihilation in polymers. *Phys. Rev. B* **2005**, *71*, 0122011–0122014.

- (12) Sato, K.; Shanai, D.; Hotani, Y.; Ougizawa, T.; Ito, K.; Hirata, K.; Kobayashi, Y. Positronium formed by recombination of positron-Electron pairs in polymers. *Phys. Rev. Lett.* **2006**, *96*, 2283021–2283024.

- (13) Sato, K.; Murakami, H.; Ito, K.; Hirata, K.; Kobayashi, Y. Probing the elemental environment around the free volume in polymers with positron annihilation age-momentum correlation spectroscopy. *Macromolecules* **2009**, *42*, 4853–4857.

- (14) Sato, K.; Baier, F.; Sprengel, W.; Würschum, R.; Schaefer, H.-E. Study of an order-disorder phase transition on an atomic scale: the example of decagonal Al-Ni-Co quasicrystals. *Phys. Rev. Lett.* **2004**, *92*, 1274031–1274034.

- (15) Yoshizawa, K.; Sato, K.; Murakami, H.; Shikazono, N.; Fujimoto, K.; Nakata, M. Open-nano pores in natural minerals studied by positron lifetime spectroscopy. *Mater. Sci. Forum* **2009**, *607*, 189–191.

- (16) Dove, P. M.; Han, N.; De Yoreo, J. J. Mechanisms of classical crystal growth theory explain quartz and silicate dissolution behavior. *Proc. Natl. Acad. Sci. U.S.A.* **2005**, *102*, 15357–15362.

- (17) Wallace, A. F.; Gibbs, G. V.; Dove, P. M. Influence of Ion-Associated Water on the Hydrolysis of Si-O Bonded Interactions. *J. Phys. Chem.* **2010**, *114*, 2534–2542.

- (18) Bakos, T.; Rashkeev, S. N.; Pantelides, S. T. Reactions and diffusion of water and oxygen molecules in amorphous SiO<sub>2</sub>. *Phys. Rev. Lett.* **2002**, *88*, 0555081–0555084.

- (19) Bakos, T.; Rashkeev, S. N.; Pantelides, S. T. H<sub>2</sub>O and O<sub>2</sub> molecules in amorphous SiO<sub>2</sub>: defect formation and annihilation mechanisms. *Phys. Rev. B* **2004**, *69*, 1952061–1952069.